AUT Journal of Electrical Engineering
10.22060/EEJ.2026.26056.6045

Bi-Level Optimization of Distributed Power Management Coordinated with Intelligent Load Shedding In Islanded Microgrid Incorporating Multi-Site Nanogrids Under Clean Energy Variability

Nour EL Yakine Kouba[1]*, Amel Brik[1], Djamel Selkim[1]

[1]Laboratory of Electrical and Industrial Systems, University of Sciences and Technology Houari Boumediene, Algiers, Algeria

nourelyakin.kouba@usthb.edu.dz, abrik2022@gmail.com, djamelselkim@gmail.com

***Corresponding Author:** nourelyakin.kouba@usthb.edu.dz

Abstract:

This paper deals with the design of an effective smart distributed management system (DMS) in islanded microgrid connected with multiple nanogrids under renewable energy variability using Fuzzy Logic method. The proposed DMS strategy was coordinated with an optimal Under-frequency Load Shedding (UFLS) to ensure power equilibrium during overloads. The recently nature-inspired named African Vultures Optimization (AVO) algorithm was employed for this purpose. The investigated microgrid includes doubly-fed induction generators (DFIG) wind farms, solar PV generators and concentrating solar power (CSP) units. Further, a storage system including Redox Flow Batteries (RFB) was used to support frequency regulation. Further, to show the validity and potential of the proposed method a variety of nanogrid systems were tested involving the sea-water desalination station, pumped solar system and electrical vehicles station. Furthermore, the proposed smart DMS coordinated with intelligent UFLS can maintain the microgrid stability using the smart deloading of the connected nanogrids using an estimated load duration curve (LDC) which minimizes the outage risk and avoids the total load shedding during faults. Using this approach, frequency stability can be maintained after disturbances. The reached results show good performances in view of frequency peak under/overshoot and settling time.

Keywords: Nanogrid, Microgrid, Renewable Energy Sources (RESs), Distributed Management System, Under-Frequency Load Shedding, Fuzzy Logic, Optimization.

10.22060/EEJ.2026.26056.6045

Abbreviations

RESs	Renewable Energy Sources
EMS	Energy Management System
DMS	Distribution Management System
HESS	Hybrid Energy Storage System
AI	Artificial Intelligence
PSO	Particle Swarm Optimization
GA	Genetic Algorithm
UFLS	Under-Frequency LoadShedding
LFC	Load Frequency Control
PID	Proportional–Integral–Derivative
AVO	AfricanVultureOptimization Algorithm
MG	Microgrid
NG	Nanogrid
ESSs	Energy Storage Systems
BMS	Battery Management System
FACTS	Flexible AC Transmission Systems
IPSO	Improved Particle Swarm Optimization
STATCOM	Static Synchronous Compensator
TCSC	Thyristor-Controlled Series Compensator
UPFC	Unified Power Flow Controller
ANFIS	Adaptive Neuro-FuzzyInference System
GWO	Grey Wolf Optimizer
DE	Differential Evolution
ES	Evolution Strategy
BBO	Biogeography-Based Optimization
CSO	Cat Swarm Optimization
GOA	Grasshopper Optimization Algorithm
PRO	Partial Reinforcement Optimizer
OPF	Optimal Power Flow
LSTM	Long Short-Term Memory
MPA	Marine Predators Algorithm
GSA	Gravitational Search Algorithm
TLBO	Teaching–Learning-Based Optimization
SHADE	Success-History based Adaptive Differential Evolution
ABC-DE	Artificial Bee Colony–Differential Evolution
EP	Evolutionary Programming
ACO	Ant Colony Optimization
ABC	Artificial Bee Colony
BA	Bat Algorithm
FFA	FireflyAlgorithm
CS	Cuckoo Search
MFO	Moth-Flame Optimization
WOA	Whale OptimizationAlgorithm
CaSO	Cat and Sparrow Optimization
TLBO	Teaching–Learning-Based Optimization
EVs	Electric Vehicles
STEP	Pumped Energy Transfer Station

PSH	Pumped-storage hydroelectricity Station
DFIG	Doubly-Fed Induction Generators
RFB	Redox Flow Batteries
CSP	Concentrating Solar Power
PV	Photovoltaic
LDC	Load Duration Curve

1. INTRODUCTION

The modern electric power system has undergone a fundamental transition from a centralized architecture dominated by large synchronous generators, to a decentralized, digitalized network integrating distributed and power electronics-interfaced resources. This transformation is driven by rising electricity demand, the diversification of energy sources, and the critical need for operational flexibility under high uncertainty. Frequency stability denotes the system's capacity to maintain equilibrium within acceptable operational limits following a generation-demand imbalance [1].

In conventional grids, immediate frequency support is provided by the rotational inertia of synchronous machines. As inverter-based renewable energy sources increasingly displace these conventional units, total system inertia is reduced, thereby weakening the grid's resistance to frequency deviations and increasing the risk of instability [2]. Thus, frequency dynamics in modern power systems exhibit faster and more severe variations, requiring more sophisticated control and coordination framework [3].

Driven by the global transition toward low-carbon energy systems, wind and solar photovoltaic generation have experienced a rapid expansion in modern power grids. Unlike conventional thermal units, these renewable energy sources (RESs) are inherently intermittent and stochastic due to their dependence on meteorological conditions. This volatility introduces frequent generation-demand mismatches that directly compromise frequency stability [4][5]. Maintaining stable operation under these conditions requires advanced control strategies and supporting technologies, such as synthetic inertia and fast frequency response mechanisms, and intelligent Under-Frequency Load Shedding, to compensate for the reduction of conventional frequency regulation capabilities [6].

Microgrids serve as fundamental architectures in modern power systems, functioning as localized energy networks that integrate multiple distributed energy resources, including renewable generation, energy storage systems, and controllable loads, within clearly defined electrical boundaries. These systems are capable of operating in both grid-connected and autonomous islanded modes [7][8]. Through the coordinated management of local resources, microgrids enhance grid reliability, improve operational flexibility, and facilitate higher penetration levels of renewable energy while preserving power quality. Furthermore, their decentralized structure enables rapid response to localized disturbances and reduces reliance on centralized utility infrastructure.

10.22060/EEJ.2026.26056.6045

Microgrid operations are typically governed by an Energy Management System (EMS), which monitors and optimizes resource utilization. The EMS ensures operational and economic efficiency by executing functions such as generation scheduling, load balancing, and stability maintenance under dynamic conditions[9]. In particular, the EMS plays a pivotal role in frequency regulation by coordinating distributed assets using advanced control frameworks and optimization techniques [10].

At a smaller scale, nanogrids have emerged as highly localized energy systems designed to supply individual buildings or discrete loads. Representing the smallest functional unit within distributed power systems, they typically consolidate local generation, storage, and demand within a restricted boundary [11]. Nanogrids can operate either independently or in coordination with microgrids and the main grid, thereby enabling flexible energy exchange and enhancing system adaptability [12]. At the distribution level, Distribution Management Systems (DMS) provide the necessary monitoring and control capabilities for these interconnected structures, ensuring secure and efficient network operation.

Within this architecture, energy storage systems, particularly Hybrid Energy Storage Systems (HESS), are central to mitigating power fluctuations effectively by combining high-power, fast-response capabilities with high-energy capacity. These systems provide rapid frequency support, compensate for transient imbalances, and improve overall system resilience [13]. As a result, the coordinated operation of nanogrids, microgrids, DMS, and storage assets establishes a more stable and flexible power system framework, particularly under high renewable penetration.

Artificial Intelligence (AI) and mathematical optimization techniques are increasingly deployed to manage the escalating complexity of modern power system operations. These methods are well suited for resolving highly nonlinear and dynamic problems, with widespread applications in forecasting, operational decision-making, and the real-time control of distributed resources. AI-based approaches, including machine learning models and intelligent control structures, enhance system adaptability and enable high-accuracy predictions of load profiles and intermittent renewable generation [14].

On the other hand, metaheuristic optimization algorithms, such as Particle Swarm Optimization (PSO) and Genetic Algorithms (GA), are widely utilized to solve complex, non-convex optimization problems, including controller parameter tuning and economic dispatch [15]. In the context of frequency stability, these intelligent and optimization-driven techniques facilitate precise tuning of control parameters, thereby improving dynamic performance and accelerating transient response times [16].

Building upon these advancements, this study investigates the integration of nanogrid architectural elements with AI-based and optimization-driven control strategies to enhance frequency stability in low-inertia power systems. This work deals with the development of a coordinated framework that optimizes frequency regulation by leveraging both distributed network architectures and intelligent optimization paradigms. Although several studies have investigated EMS, load frequency control, and load shedding

10.22060/EEJ.2026.26056.6045

independently, limited attention has been paid to the coordinated operation of intelligent DMS-UFLS strategies in interconnected microgrid–nanogrid systems under renewable uncertainty.

Although considerable research has been devoted to frequency regulation, renewable-energy integration, energy management, and emergency control, these functions are generally investigated separately or with limited coordination between primary/secondary frequency control and emergency actions. Existing studies mainly focus on improving LFC performance, optimizing energy-storage operation, or developing DMS/UFLS strategies, while the simultaneous coordination of these functions under renewable-energy variability and severe disturbances remains insufficiently investigated. In particular, there is a need for an adaptive framework that can determine the appropriate contribution of conventional generation, distributed energy resources, and energy storage according to the instantaneous frequency and active-power conditions of the interconnected system.

To address this research gap, this study proposes an integrated LFC–DMS/UFLS coordination framework for interconnected microgrids with renewable energy sources and energy storage systems. The proposed approach combines a fuzzy-PID controller with a metaheuristic optimization technique and an intelligent DMS/UFLS strategy. Unlike approaches that independently optimize frequency regulation or emergency load shedding, the proposed method coordinates these control levels according to frequency deviation, active-power deviation, and the available conventional LFC capacity. Consequently, the proposed framework provides a coordinated response to different operating conditions, including power imbalance, renewable-energy fluctuations, and severe disturbances, with the objective of improving frequency stability while reducing the dependence on conventional generation. The main differences between the proposed approach and representative existing studies are summarized in Table 1.

The main contributions of this work are:

- Development of an intelligent EMS tool for interconnected multi-nanogrids;
- Development of an intelligent distributed DMS tool for nanogrid;
- Development of an intelligent Load Shedding (UFLS) tool for multi-nanogrids system;
- Integration of AVO and fuzzy-logic for multi-NG coordination;
- Evaluation of the contribution of storage devices in improving system frequency stability.

Table.1. Comparative Literature Review Table.

References	EMS	DMS	UFLS	Control	ESS	FACTS	AI	Optimization
[1]	✗	✗	✓	✓	✓	✗	✗	✓
[2]	✗	✗	✗	✓	✗	✗	✗	✓
[3]	✗	✗	✗	✓	✗	✗	✗	✓
[4]	✗	✗	✗	✓	✓	✓	✓	✓
[5]	✗	✗	✓	✓	✗	✗	✗	✗
[6]	✗	✗	✗	✓	✗	✗	✗	✗
[7]	✓	✓	✗	✓	✓	✗	✗	✓

10.22060/EEJ.2026.26056.6045

[10]	✓	✗	✗	✓	✓	✗	✗	✓
[13]	✓	✗	✗	✗	✓	✗	✗	✓
[14]	✗	✗	✗	✓	✓	✗	✓	✓
[16]	✓	✗	✗	✓	✓	✗	✓	✓
[18]	✗	✗	✗	✗	✓	✗	✓	✗
[21]	✓	✗	✗	✗	✓	✗	✗	✓
[22]	✓	✓	✗	✗	✓	✗	✓	✓
[23]	✓	✗	✗	✗	✓	✗	✓	✓
[24]	✓	✗	✗	✗	✓	✗	✓	✓
[26]	✗	✗	✗	✗	✗	✓	✗	✓
[29]	✗	✗	✗	✗	✗	✓	✗	✓
[30]	✗	✗	✗	✗	✗	✓	✓	✓
[31]	✗	✗	✗	✗	✗	✓	✗	✓
This work	✓	✓	✓	✓	✓	✓	✓	✓

✓**present;** ✗**not present;**

The rest of this paper is organized as follows. Section 2 reviews the recent related literature. While Section 3 presents the detailed system modeling of the microgrid-nanogrid network. Section 4 showcases the proposed framework, detailing the control architecture and optimization paradigms. Section 5 provides the simulation setup and the comprehensive case studies, and the discussion of the results under operational scenarios. Section 6 presents future work and envisaged perspectives. Finally, Section 7 concludes the paper and outlines prospective avenues for future research.

2. LITTERATURE REVIEW

The evolution of smart grids is fundamentally driven by the need to efficiently integrate RESs, thereby enhancing system flexibility and ensuring network reliability under increasing stochastic uncertainty. Energy storage systems (ESSs), particularly battery-based technologies, serve as critical assets for load balancing and frequency regulation. To maximize the utility of these assets, AI-driven Battery Management Systems (BMS) have emerged as a key mechanism to optimize battery performance, safety and operational lifespan through advanced estimation and control frameworks. Recent literature have focused on leveraging deep learning architectures and data-driven methodologies for accurate state estimation and predictive maintenance.

For instance, a deep learning framework was proposed in [17] for the real-time estimation of lithium-ion batteries state-of-health, whereas neural-network-based approaches were developed in [18] to achieve for accurate state-of-charge estimation under dynamic operating conditions. Furthermore, the application of AI-driven digital twins for intelligent battery management was investigated [19], and a comprehensive review recent advancements in intelligent BMS architectures tailored for grid-scale storage deployment was provided in [20].

Nanogrids have attracted research interest as highly localized systems capable of operating autonomously or in coordination with larger grid structures, thereby offering superior resilience and efficiency for distributed energy applications. Managing their heterogeneous integration of distributed generation, energy storage, and flexible loads requires sophisticated strategies to ensure multi-objective optimization. Contemporary literature emphasizes the deployment of AI, distributed optimization paradigms, and real-time control techniques to augment nanogrid performance. For instance, an AI-based energy management framework was proposed in [21] for grid-connected nanogrids during anomalous demand profiles, successfully coordinating renewable assets and storage systems. Similarly, a multi-agent system structure was developed [22] for the cooperative control of interconnected nanogrids, effectively improving system stability and collaborative energy sharing. Moreover, neural network-based scheduling methodologies for optimal nanogrid dispatch were investigated in [23], while reinforcement learning frameworks were explored in reference [24] to facilitate adaptive energy management within small-scale distributed grid systems. AI is transforming how electrical grids maintain frequency and voltage stability, especially as RESs introduce variability and uncertainty. Traditional controllers, such as PID controllers, struggle to adapt in real time to rapid fluctuations caused by high penetrations of wind and solar generation, resulting in degraded frequency performance and power quality. AI techniques such as deep learning, reinforcement learning, and adaptive neuro-fuzzy systems enable predictive and self-optimizing control devices to mitigate frequency deviations and voltage sags. AI-based adaptive controllers have demonstrated superior real-time responsiveness and robustness in high-renewable scenarios, enabling enhanced dynamic stability, reduced harmonic distortion, and improved active/reactive power regulation compared to conventional schemes. These capabilities are critical for modern grid stability because fluctuating renewable integration reduces system inertia and increases the likelihood of frequency excursions, making intelligent control indispensable for reliable grid operation [25].

In recent years, a variety of optimization approaches have been developed and applied to enhance the control, placement, and parameter tuning of FACTS devices for frequency and dynamic stability in power systems with high renewable penetration. In [26], a hybrid Genetic Algorithm–Improved Particle Swarm Optimization (GA-IPSO) framework was proposed to simultaneously optimize the sizes and locations of STATCOM, TCSC, and UPFC devices, demonstrating reduced power losses and operating cost compared to standalone methods. In [27], hybrid AI-optimized ANFIS controllers were introduced to enhance small-signal and transient stability for multi-machine systems by combining GA, PSO, and Grey Wolf Optimizer (GWO) for multi-objective damping performance. In [28] the authors classified various metaheuristic and evolutionary methods used for FACTS optimization (including Differential Evolution (DE), Evolutionary

Strategies (ES), Biogeography-Based Optimization (BBO), Cat Swarm Optimization (CSO), and Grasshopper Optimization Algorithm (GOA)), highlighting improvements in voltage profile and loss reduction across standard test systems. Additionally, Partial Reinforcement Optimizer (PRO) has been proposed for simultaneous optimal placement and rating of multi-type FACTS devices in OPF contexts [29]. Emerging research integrates deep learning controllers (e.g., LSTM) for real-time dynamic control optimization under uncertainty, showing superior performance compared to static heuristics [30]. In [31], comparative studies show performance differences among Marine Predators Algorithm (MPA), Gravitational Search Algorithm (GSA), TLBO, and hybrid methods such as Success History-Based Adaptive Differential Evolution (SHADE) and ABC-DE, with different strengths in loss minimization and cost reduction. A critical review in [32] categorizes dozens of optimization techniques applied to FACTS problems, including Genetic Algorithm (GA), Evolutionary Programming (EP), Ant Colony Optimization (ACO), Artificial Bee Colony (ABC), Bat Algorithm (BA), Firefly Algorithm (FFA), Cuckoo Search (CS), Moth-Flame Optimization (MFO), Whale Optimization (WOA), Cat Swarm Optimization (CaSO), and Teaching-Learning-Based Optimization (TLBO).

A careful review of the recent literature reveals that most existing studies address EMS and under-frequency load shedding as independent problems, with limited coordination among these functions [33]. Although AI-based controllers and optimization algorithms have demonstrated promising performance for frequency regulation, few works have investigated their joint application within interconnected microgrid–nanogrid architectures incorporating diverse RESs, energy storage devices, and flexible loads under renewable uncertainty. Furthermore, existing approaches rarely exploit hierarchical distributed management strategies capable of simultaneously enhancing power balance, frequency stability, and load prioritization. This research addresses these gaps by proposing a coordinated bi-level DMS-UFLS framework based on fuzzy logic and African Vultures Optimization for resilient operation of islanded multi-nanogrid systems.

3. SYSTEM MODELING

The fidelity of a frequency stability analysis hinges on the mathematical coherence of its underlying components. Within interconnected microgrid-nanogrid architectures, the diverse range of power-electronics-interfaced resources introduces complex dynamic interactions that must be captured with a high degree of precision. In this section, a unified modeling framework that balances computational efficiency with the physical rigor required to represent the electrical and mechanical characteristics of the subsystems is introduced. Specifically, mathematical formulations are presented for the main subsystems under consideration: photovoltaic arrays, DFIG-based wind turbines, RFB energy storage systems, electric vehicles (EVs), desalination facilities, and pumped-storage hydroelectric units. Fig.1 illustrates the comprehensive system topology analyzed in this study, highlighting the integration of the coordinated DMS-UFLS frame work driven by artificial intelligence and optimization algorithms.

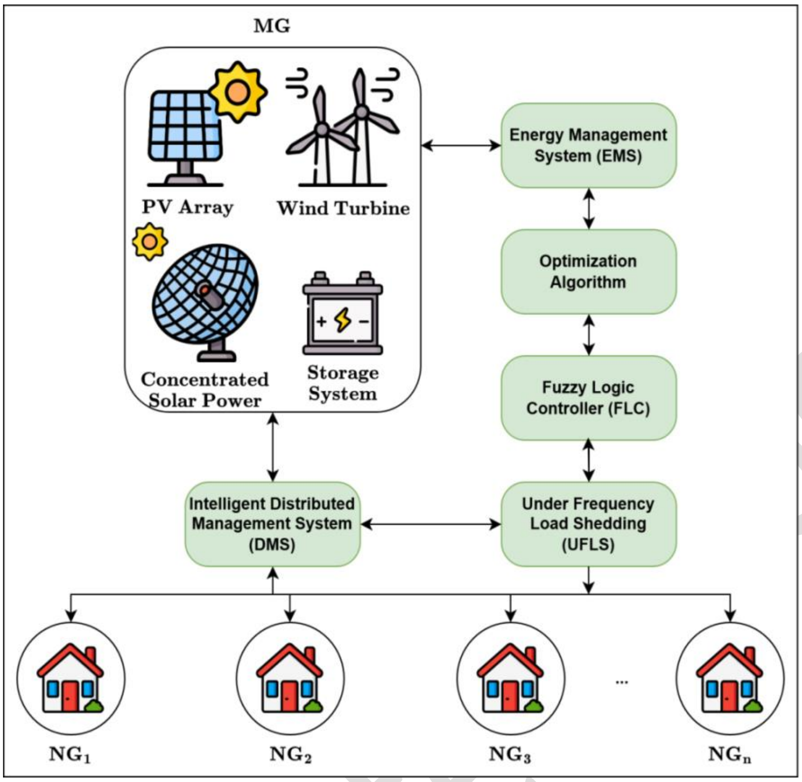

Fig 1. Proposed Multi-Microgrid-Nanogrids (MMNGs) System.

3.1. Photovoltaic Array Model

Photovoltaic systems utilize semiconductor materials to convert solar irradiance into electricity, serving as a scalable cornerstone for microgrid and nanogrid architectures. However, the electrical output of PV systems is inherently nonlinear and strongly dependent on environmental conditions such as solar irradiance and cell temperature [32]. Among the various modeling approaches available, the single-diode five-parameter model is widely adopted due to its good balance between accuracy and computational simplicity. This model represents the PV cell using an equivalent circuit composed of a current source, a diode, and series and shunt resistances, allowing precise characterization of the current–voltage and power–voltage characteristics under varying operating conditions [34]. This model was used for both PV and CSP units.

The output current of a PV cell based on the five-parameter single-diode model is expressed as:

$$I = I_{ph} - I_0[\exp\left(\frac{V + IRs}{n_d.V_t}\right) - 1] - \frac{V + IRseries}{Rshunt} \quad (1)$$

where, I and V are the output current and voltage of the PV cell, respectively; I_{ph} is the photo-generated current, which depends on solar irradiance and temperature; I_0 is the diode saturation current; R_{series} and

R_{shunt} are the series and shunt resistances; n_d is the diode ideality factor; and V_t is the thermal voltage, given by:

$$V_t = \frac{kT_{cell}}{q} \tag{2}$$

with, k being the Boltzmann constant, T_{cell} the cell temperature in *Kelvin*, and q the electron charge.

The photo-current I_{ph} is typically modeled as a function of irradiance and temperature, while the saturation current I_0 varies exponentially with temperature. This model can be extended from a single cell to a PV module or array by considering the number of cells connected in series and parallel. Due to its ability to accurately capture the nonlinear behavior of PV systems under varying environmental conditions, the five-parameter model is widely used in simulation studies and control-oriented applications in modern power systems [35].

3.2. Wind Turbine Model

Wind energy has become a major component of modern power systems due to its maturity, large-scale deployment, and compatibility with distributed generation architectures such as microgrids and nanogrids. While wind turbines offer efficient variable-speed operation, their integration is complicated by the stochastic nature of wind, which directly impacts grid frequency regulation [36]. Among the various generator technologies, the DFIG is widely used in variable-speed wind turbines due to its ability to operate efficiently over a wide range of wind speeds while allowing independent control of active and reactive power. The DFIG-based model provides a suitable balance between modeling accuracy and computational efficiency, making it a standard choice for power system studies [37].

The aerodynamic power extracted from the wind turbine is given by:

$$P_t = \frac{1}{2}\rho_{air} \mathrm{A} v^3 C_p(\lambda, \beta) \tag{3}$$

where, ρ_{air} is the air density, A is the swept area of the turbine blades, v is the wind speed, and C_p is the power coefficient, which depends on the tip-speed ratio λ and blade pitch angle β. The tip-speed ratio is defined as:

$$\lambda = \frac{w_t R_b}{v} \tag{4}$$

where, ω_t is the turbine rotational speed and R_b is the blade radius.

The mechanical dynamics of the turbine-generator system can be described by:

$$J\frac{dw_r}{dt} = T_m - T_e \tag{5}$$

where, J is the combined inertia of the turbine and generator, ω_r is the rotor speed, T_m is the mechanical torque derived from wind power, and T_e is the electromagnetic torque.

The electrical behavior of the DFIG is commonly modeled in the synchronous dq reference frame using the following voltage equations:

$$v_{ds} = R_s.i_{ds} + \frac{d\psi_{ds}}{dt} - w_s\Psi_{qs} \tag{6}$$

$$v_{qs} = R_s.i_{qs} + \frac{d\psi_{qs}}{dt} - w_s\Psi_{ds} \tag{7}$$

$$v_{dr} = R_r.i_{dr} + \frac{d\psi_{dr}}{dt} - (w_s - wr)\Psi_{qr} \tag{8}$$

$$v_{qr} = R_r.i_{qr} + \frac{d\psi_{qr}}{dt} - (w_s - wr)\Psi_{dr} \tag{9}$$

where, v, i, and ψ represent voltages, currents, and flux linkages in the stator (s) and rotor (r) circuits, respectively; R_s and R_r are stator and rotor resistances; and ω_s is the synchronous angular speed.
The electromagnetic torque is expressed as:

$$T_e = \frac{3}{2}.\frac{P}{2}(\Psi_{ds}i_{qs} - \Psi_{qs}i_{ds}) \tag{10}$$

where, P is the number of poles. This model enables independent control of active and reactive power through rotor-side converters, which is essential for frequency support and voltage regulation in modern grids [38].

3.3. Redox Flow Batteries Model

Redox flow batteries distinguish themselves from conventional solid-state batteries by decoupling power and energy capacity through the use of external electrolyte tanks, allowing independent scaling of power (stack size) and energy capacity (tank volume). This unique feature makes them particularly suitable for applications in microgrids and nanogrids, where they can support renewable energy integration, enhance system flexibility, and contribute to frequency stability [39]. In addition, RFB offer fast response capabilities, making them effective for mitigating power fluctuations and providing ancillary services. Electrochemical-based models provide high accuracy but are often complex; thus, simplified dynamic models that capture the essential electrical behavior are commonly used in system-level studies [40]. The terminal voltage of a redox flow battery can be expressed as a function of its open-circuit voltage and internal losses:

10.22060/EEJ.2026.26056.6045

$$V_{RFB} = E_{oc-RFB} - R_{\text{int\_}RFB} . I_{RFB} \tag{11}$$

where, V_{RFB} is the terminal voltage, E_{oc_RFB} is the open-circuit voltage, R_{int_RFB} represents the internal resistance of the battery, and I_{RFB} is the RFB's charge/discharge current.

The open-circuit voltage is typically modeled using the Nernst equation:

$$E_{oc-RFB} = E^0 + \frac{RT}{nF} \ln\left(\frac{C_{ox}}{C_{red}}\right) \tag{12}$$

where, E^0 is the standard cell potential, R is the universal gas constant, T is the temperature, n is the number of electrons transferred in the reaction, F is Faraday's constant, and C_{ox} , C_{red} are the concentrations of oxidized and reduced species, respectively.
The state of charge (SOC) of the RFB is governed by:

$$\frac{dSOC_{RFB}}{dt} = -\frac{I_{RFB}}{Q_{nom\_RFB}} \tag{13}$$

where, Q_{nom_RFB} is the nominal capacity of the battery. The SOC reflects the available energy stored in the electrolyte and directly influences the open-circuit voltage and system performance.

To account for dynamic behavior, additional elements such as polarization losses and flow dynamics can be included, but for most power system applications, the above model provides a sufficient representation of the RFB's electrical characteristics [41].

3.4. Electric Vehicles Model

Aggregated EV fleets function as mobile energy storage units, capable of providing Vehicle-to-Grid (V2G) services such as peak shaving and frequency regulation. Their fast response and widespread availability make them particularly valuable in microgrid and nanogrid environments with high renewable energy penetration [42]. However, the stochastic nature of EV availability, driven by user behavior and mobility patterns, introduces additional uncertainty in system operation [43].
The electrical behavior of an EV battery can be represented using a simplified equivalent circuit model, where the terminal voltage is expressed as:

$$V_{EV} = E_{OC\_EV} - R_{\text{int\_}EV} . I_{EV} \tag{14}$$

where, V_{EV} is the battery terminal voltage, E_{oc_EV} is the open-circuit voltage of the EV, R_{int_EV} is the internal resistance of the EV, and I_{EV} is the EV's charge/discharge current. The state of charge dynamics are given by:

10.22060/EEJ.2026.26056.6045

$$\frac{dSOC_{EV}}{dt} = -\frac{I_{EV}}{Q_{nom\_EV}} \tag{15}$$

where, Q_{nom_EV} represents the nominal capacity of the EV battery. The SOC reflects the available energy in the battery and determines the operational limits for charging and discharging processes. The power exchanged between the EV and the grid is defined as:

$$P_{EV} = V_{EV} . I_{EV} \tag{16}$$

which can be controlled to either absorb energy (charging mode) or inject energy back into the grid (V2G mode). In aggregated models, a fleet of EVs is often represented as a controllable power source or sink with constraints on total capacity, SOC limits, and availability patterns. Due to their flexibility and fast response, EVs can significantly contribute to frequency stability by providing short-term power support and balancing supply-demand mismatches. Their integration into advanced energy management systems enables coordinated control strategies that enhance grid reliability and efficiency, particularly in low-inertia systems with high renewable energy penetration [44].

3.5. Desalination Station Model

Desalination stations are increasingly integrated into modern power systems, particularly in regions facing water scarcity, where they represent significant and controllable electrical loads. These systems convert seawater or brackish water into potable water, with Reverse Osmosis (RO) being the most widely used technology due to its relatively high efficiency and modularity [45]. From a power system perspective, desalination plants exhibit high energy consumption and can operate flexibly within certain limits, making them suitable for demand-side management and grid support applications. In microgrid and nanogrid environments, desalination stations can be coordinated with renewable generation and storage systems to improve overall system stability and energy utilization [46]. The power consumption of a reverse osmosis desalination unit can be expressed as:

$$P_{des} = \frac{Q_W . \Delta P}{\eta_{sys}} \tag{17}$$

where, P_{des} is the electrical power consumed by the desalination system, Q_w is the water flow rate, ΔP is the pressure difference across the membrane, and η_{sys} represents the overall system efficiency, including pump and motor efficiencies. The pressure required for the RO process depends on the osmotic pressure and operating conditions, typically modeled as:

$$\Delta P = P_{osm} + P_{loss} \tag{18}$$

where, P_{osm} is the osmotic pressure of the feedwater and P_{loss} accounts for hydraulic losses in the system.

10.22060/EEJ.2026.26056.6045

The produced freshwater flow rate is related to the input conditions by:

$$Q_{prod} = \eta_{rec} . Q_{in} \tag{19}$$

where, Q_{prod} is the permeate (freshwater) flow rate, Q_{in} is the feed water flow rate, and η_{rec} is the recovery ratio of the desalination process.

From a dynamic perspective, desalination plants can be modeled as controllable loads with operational constraints such as minimum and maximum power limits, ramp rates, and water demand requirements. Their power consumption can be adjusted within these constraints to support grid operation, for instance by reducing load during frequency drops or increasing consumption during excess generation periods [47][48][49].

3.6. Pumped-Storage Hydroelectricity Station Model

Pumped-storage hydroelectricity (PSH) is one of the most mature and widely deployed large-scale energy storage technologies, playing a crucial role in modern power systems by providing energy balancing, peak shaving, and frequency regulation services [50]. A PSH system operates by storing energy in the form of gravitational potential energy: water is pumped from a lower reservoir to an upper reservoir during periods of excess generation, and released through turbines to generate electricity during periods of high demand. Due to its high capacity, fast response, and long operational lifetime, PSH is particularly suitable for supporting systems with high penetration of renewable energy sources. In microgrid and nanogrid contexts, PSH can act as a central balancing unit, enhancing system flexibility and contributing to frequency stability [51].

The power generated by the hydro turbine in generation mode is given by:

$$P_{gen} = \eta_t . \rho_{water} . g . h . Q \tag{20}$$

where, P_{gen} is the generated electrical power, η_t is the turbine-generator efficiency, ρ_{water} is the water density, g is the gravitational acceleration, h is the effective hydraulic head, and Q is the water flow rate.

In pumping mode, the electrical power consumed is expressed as:

$$P_{pump} = \frac{\rho_{water} . g . h . Q}{\rho_p} \tag{21}$$

where, η_p is the efficiency of the pump-motor unit.

The dynamic behavior of the water flow can be approximated by:

$$\frac{dQ}{dt} = \frac{1}{T_W}(Q_{ref} - Q) \tag{22}$$

10.22060/EEJ.2026.26056.6045

where, Q_{ref} is the reference flow rate and T_w is the water starting time constant, representing the inertia of the water column in the penstock.

The state of energy stored in the upper reservoir can be described by:

$$\frac{dE}{dt} = P_{pump} - P_{gen} \tag{23}$$

which reflects the balance between pumping and generating operations.

In power system studies, PSH plants are often modeled as controllable units capable of switching between generation and pumping modes, subject to operational constraints such as reservoir limits, ramp rates, and efficiency losses. Their fast response and large capacity enable them to provide effective frequency support by rapidly adjusting power output or consumption in response to system imbalances [52].

4. PROPOSED STRATEGY

The shift in the literature toward hybrid and neural-metaheuristic frameworks reflects an integration of heuristic search, evolutionary computation, and artificial intelligence to move beyond classical optimization [53]. These advanced methodologies are now extensively employed for optimal device sizing, placement, and controller parameter tuning because they effectively balance convergence speed with the high degree of adaptability required to navigate the nonlinear dynamics and inherent variability of modern renewable-rich power grids. Fig.2, presents the main contribution of the developed Bi-Level optimal DMS-UFLS to enhance dynamic microgrid behaviors in case of multiple nanogrids and multi-load variability. Two stage have been employed. The first stage includes an optimal load frequency control loop based on a combined Fuzz-PID controller optimize via the recently African Vultures Optimization (AVO) algorithm, where, the second stage involves an intelligent DMS using fuzzy logic method coordinated with optimal UFLS and ESS that was installed to ensure power equilibrium and support frequency regulation, a step-by-step flowchart of the DMS-UFLS coordination algorithm is given in Appendix.

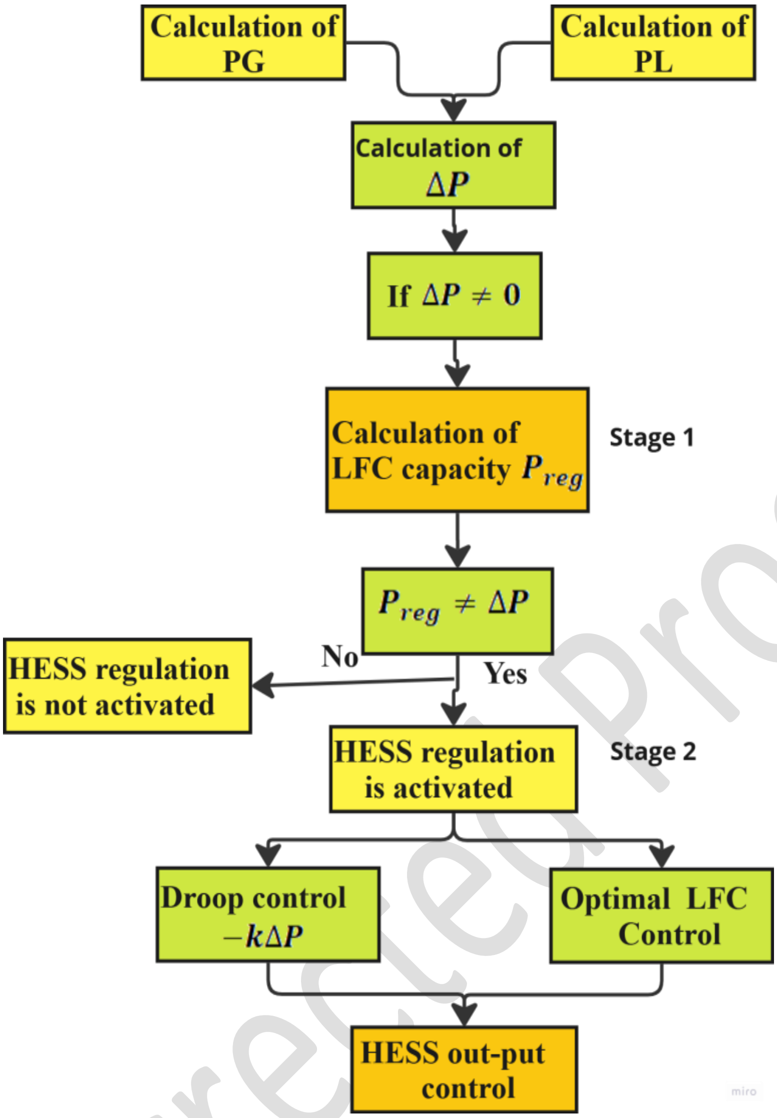

Fig 2. Proposed Bi-Level Optimal DMS-UFLS Strategy.

The integration of renewable energy sources and distributed elements in modern power systems increases operational complexity and introduces significant uncertainties, particularly in microgrid and nanogrid environments. Ensuring frequency stability and efficient energy utilization therefore requires advanced and adaptive control strategies. Conventional methods often struggle under such dynamic conditions, which has led to the growing adoption of intelligent techniques. In this context, fuzzy logic control provides a flexible and robust solution for handling nonlinearities and uncertainties. In this study, the LFC loop is implemented using a fuzzy logic-based PID controller, while energy management is achieved through a fuzzy logic-based EMS, enabling coordinated and efficient system operation that combine both of DMS and UFLS.

In modern microgrids, LFC is vital for balancing generation and demand to ensure frequency stability, where high renewable penetration and reduced inertia complicate regulation. Energy storage systems, such as batteries and pumped-storage units, are frequently employed to mitigate these power

10.22060/EEJ.2026.26056.6045

imbalances due to their rapid, bidirectional response. To optimize performance in these dynamic settings, this study implements a hybrid fuzzy logic-based PID controller that overcomes the limitations of conventional, fixed-parameter PID methods. While classical PID controllers are valued for their simplicity, they often struggle with the intermittency of RES; by incorporating fuzzy logic, the controller can adaptively tune PID gains based on frequency deviations without requiring an exact mathematical model. This integrated approach enhances the coordination of storage units, providing superior robustness, faster settling times, and reduced overshoot in low-inertia environments.

The DMS is essential for coordinating generation units, storage systems, and loads to ensure efficient operation and stability within microgrids, especially when balancing the variability of high renewable energy penetration. Given that traditional optimization methods often struggle with the nonlinearities and modeling difficulties inherent in these systems, this study adopts a fuzzy logic-based DMS as shown in Fig.3. This approach leverages heuristic, rule-based reasoning rather than precise mathematical models, allowing for real-time decision-making based on variables such as load demand and power availability. By dynamically allocating resources and prioritizing energy usage, the fuzzy-based DMS provides superior flexibility and robustness compared to conventional techniques, ultimately enhancing energy utilization and supporting frequency stability in complex microgrid and nanogrid environments.

In this aim, two fuzzy logic methods were used,. In Level 1, the Mamdani fuzzy inference system was used to design the intelligent Fuzzy-PID controller, whose parameters were optimally tuned using the African Vultures Optimization algorithm using the ITAE criterion as the objective function. Further, the Sugeno fuzzy inference system was adopted for the DMS and UFLS actions.

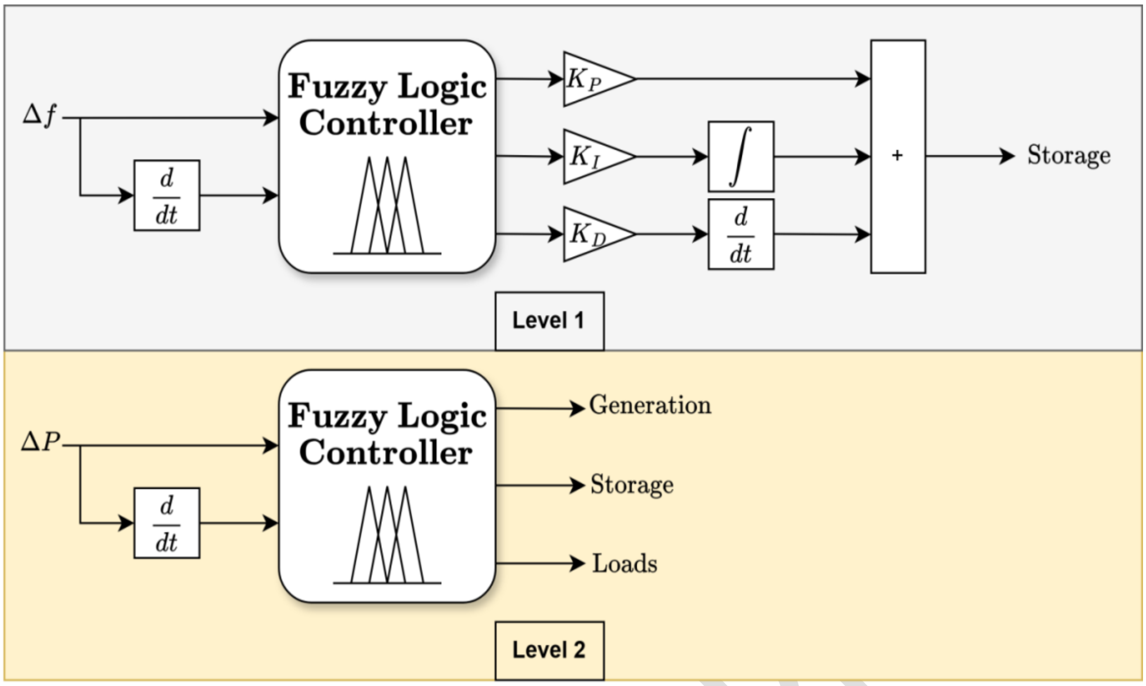

Fig 3. Proposed Optimal Fuzzy and Fuzzy-PID Controllers.

The performance of any optimization algorithm strongly depends on the formulation of an appropriate objective function. In power system optimization problems, the objective function serves as a quantitative measure of system performance and guides the search process toward the most suitable solution. For load frequency control applications, the objective function must accurately reflect the dynamic behavior of the system following disturbances, including frequency deviations, oscillations, and settling characteristics. Therefore, selecting a performance index capable of penalizing undesirable transient responses is essential to ensure both stability and robustness in renewable-rich microgrids.

As presented in Figs 2 and 3, the proposed approach is based on three key variables: frequency deviation (Δf), active power deviation (ΔP), and the available conventional secondary Load Frequency Control (LFC) capacity**.** The coordination mechanism is implemented through two sequential Levels :

In Level 1 , only the optimal Fuzzy-PID LFC controller is activated. First, the active power deviation is calculated as the difference between the total generated power and the total load demand. If $\Delta P = 0$, the system is in equilibrium and no control action is required. If $\Delta P > 0$, the system experiences surplus generation and the generated power must be reduced by minimizing the generated power from the renewable sources, here the first output of the fuzzy logic act as MPPT device. Conversely, if $\Delta P < 0$, the system is overloaded, and additional power support is required from the energy storage system (ESS). The ESS receives two control inputs in the proposed architecture. The first input is dedicated to frequency regulation (LFC), while the second input is responsible for energy management through charging and discharging

cycles. During the first stage, the frequency regulation input is activated including power generation management. Initially, the droop controller provides a fast primary frequency response to stabilize the system and estimate the exact power support required from the ESS. Simultaneously, the fuzzy controller maximizes the contribution of renewable energy sources to reduce the burden on conventional generators.

Once the system reaches the second operating stage, Level 2 (DMS/EMS) is activated. At this level, the second ESS control input manages the charging and discharging process to maintain power balance and achieve smoother frequency restoration. In addition, under severe or multiple load disturbances, when the available LFC reserve and ESS support become insufficient, the proposed strategy automatically switches to the Under-Frequency Load Shedding (UFLS) scheme to disconnect selected loads and restore the generation-demand balance. In summary, the proposed framework employs two coordinated fuzzy logic agents. The first fuzzy agent is dedicated exclusively to LFC-based frequency regulation through the ESS. The second fuzzy agent performs three coordinated functions:

- Maximizing renewable power generation,
- Managing the secondary LFC support through the ESS,
- Activating the UFLS mechanism when necessary.

This hierarchical coordination ensures an efficient transition between frequency control, energy management, and emergency load shedding, thereby enhancing the stability and resilience of the interconnected multi-nanogrid system. In this purpose, two fuzzy logic methods were used, as described in Table 2 and Table 3. In Level 1, the Mamdani fuzzy inference system was used to design the intelligent Fuzzy-PID controller, whose parameters were optimally tuned using the African Vultures Optimization algorithm using the Integral of Time-weighted Absolute Error (ITAE) criterion as the objective function. In contrast, the Sugeno fuzzy inference system was adopted for the DMS and UFLS actions.

In this paper, ITAE criterion was selected as the objective function due to its effectiveness in minimizing long-duration frequency deviations. Unlike conventional indices such as IAE, ISE, and ITSE, the ITAE criterion assigns a higher penalty to errors that persist for longer periods, thereby encouraging faster damping and shorter settling times. This characteristic makes ITAE particularly suitable for islanded microgrids with high renewable energy penetration, where rapid frequency restoration is critical to maintaining system stability. Consequently, the AVO algorithm was employed to determine the optimal parameters of the proposed Fuzzy-PID controller by minimizing the following objective function:

$$fit = \int_0^t t.(|\Delta f| + |\Delta P|)dt \tag{24}$$

The decision variables of the optimization problem are the proportional, integral and derivative gains of the Fuzzy-PID controller. The AVO algorithm searches for the optimal controller parameters that minimize the ITAE performance index while ensuring stable operation of the microgrid under renewable generation and load disturbances. The range of the controller parameters are selected between a given lower bound (LB) and upper bound (UB), Subject to:

$$\begin{cases} K_{p\_\min} \le K_p \le K_{p\_\max} \\ K_{i\_\min} \le K_i \le K_{i\_\max} \\ K_{d\_\min} \le K_d \le K_{d\_\max} \end{cases} \tag{25}$$

$$\begin{cases} K_{e\_\min} \le K_e \le K_{e\_\max} \\ K_{ce\_\min} \le K_{ce} \le K_{ce\_\max} \end{cases} \tag{26}$$

The effectiveness of the proposed bi-level control strategy depends on the proper design of the fuzzy inference systems employed in both the LFC loop and the DMS. The fuzzy controllers were developed using expert knowledge and heuristic rules to handle the nonlinear and uncertain operating conditions introduced by renewable energy variability and load fluctuations. In the first control level, the Fuzzy-PID controller dynamically adjusts the control action according to the frequency deviation (*Δf*) and its rate of change (*dΔf/dt*), ensuring rapid frequency restoration and improved dynamic performance. In the second control level, the fuzzy-based DMS determines the appropriate management and load-shedding actions based on the system operating conditions to maintain power balance and enhance overall microgrid stability. The rule bases adopted for both fuzzy controllers are summarized in Tables 2 and 3.

Table 2. Fuzzy Logic Controller Rule Table used in Level 1.

dΔf/dt \ Δf	**NB**	**NS**	**ZE**	**PS**	**PB**
NB	NB	NB	NB	NS	ZE
NS	NB	NB	NS	ZE	PS
ZE	NB	NS	ZE	PS	PB
PS	NS	ZE	PS	PB	PB
PB	ZE	PS	PB	PB	PB

Table 3. Fuzzy Logic Controller Rule Table used in Level 2.

dΔP/dt \ ΔP	**NB**	**NS**	**ZE**	**PS**	**PB**
NB	ON	ON	ON	ON	OFF
NS	ON	ON	ON	OFF	OFF
ZE	ON	ON	OFF	ON	ON
PS	OFF	OFF	ON	ON	ON
PB	OFF	ON	ON	ON	ON

5. SIMULATION RESULTS

This section presents the simulation results of the investigated microgrid connected multi-nanogrids presented in Fig.4. A multi-sources microgrid was simulated under various scenarios to show the contribution of the proposed optimal coordinated DMS-UFLS in case of Multi-Site Nanogrids. In the first simulation the system was simulated only with the LFC loop without the contribution of the proposed strategy, then in the second simulation the ESS was considered to support both DMS and LFC loop in coordination with UFLS.

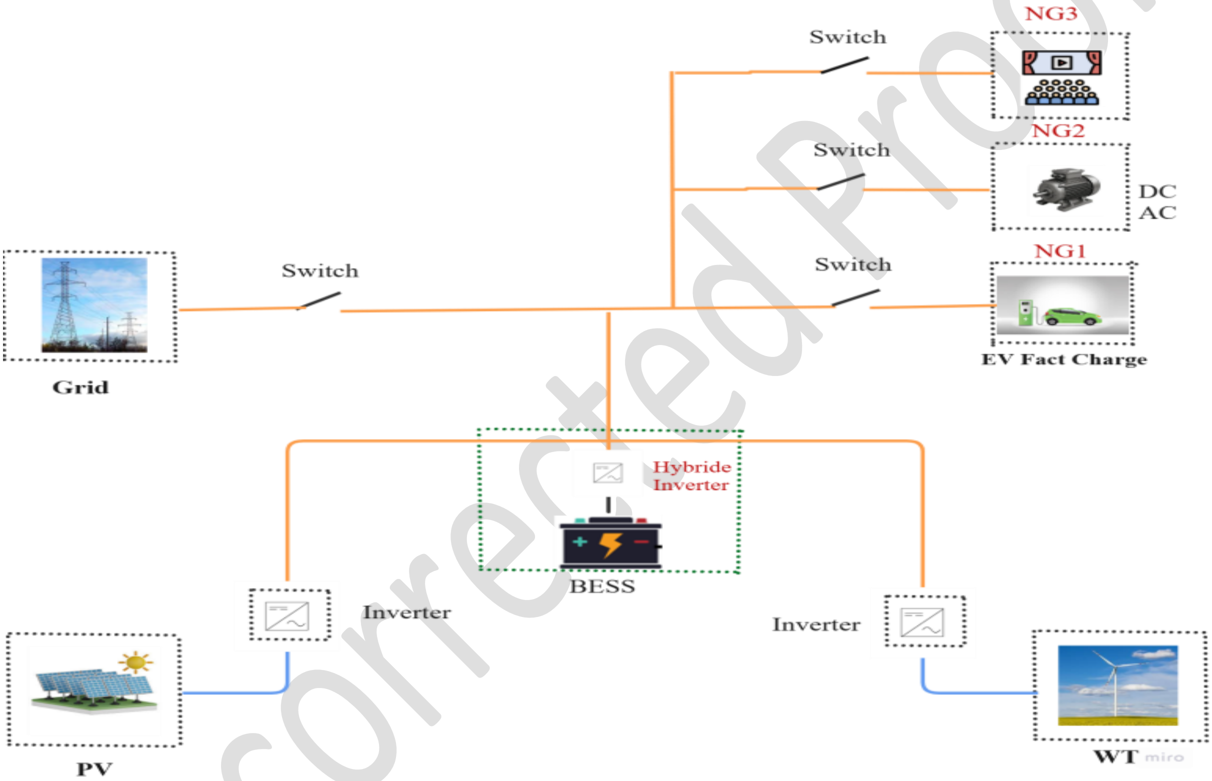

Fig 4. Bi-Level Optimal DMS Coordinated UFLS Method.

To evaluate the effectiveness of the proposed optimal coordinated DMS-UFLS strategy, two simulation cases were performed on the interconnected renewable-based microgrid–multi-nanogrid system illustrated in Fig.4. The central microgrid integrates three renewable energy sources, namely PV arrays, wind turbines, and concentrated solar power station, which collectively supply the network under varying operating conditions. A Redox Flow Battery device is incorporated as the energy storage system to compensate for renewable intermittency and provide fast power support during transient events. The microgrid is interconnected with three nanogrids through bidirectional power exchange. The first nanogrid supplies an EV charging station characterized by highly variable charging demand. The second nanogrid is dedicated to a seawater desalination station, representing a relatively constant but high-power industrial load. The third nanogrid consists of a STEP station, which operates as a flexible energy storage unit by storing surplus renewable energy during low-demand periods and supplying power during generation deficits. In both simulation cases, the interconnected system initially operates under steady-state conditions at the nominal frequency of 50 Hz, where the combined power generated by the PV arrays, WTs, and CSP plant satisfies the aggregated demand of the three nanogrids. A load disturbance is subsequently introduced to create an active power imbalance between generation and demand. The dynamic response of the system is evaluated in terms of frequency deviation, generated power, load demand, and power imbalance. The two simulation cases differ only in the activated control strategy, thereby allowing a direct assessment of the contribution of the proposed coordinated DMS-UFLS and ESS. Before t = 0 s, the system is allowed to reach steady state. At t = 0 s, a load disturbance is introduced in the form of either a sudden load increase, a reduction in renewable generation. The simulation was conducted during 5 min (300 s) to show the effect of primary and secondary frequency control loops.

In the first simulation case, the interconnected system comprising the PV arrays, wind turbines, CSP plant, RFB, EV charging nanogrid, desalination nanogrid, and STEP nanogrid operates with only the conventional LFC loop enabled. Although the RFB and STEP are physically integrated into the system architecture, they do not participate in frequency regulation or energy management, and the proposed coordinated DMS-UFLS strategy is disabled. After the system reaches its initial steady-state operating point, a load disturbance is introduced, producing a mismatch between the available renewable generation and the aggregated demand of the three nanogrids. Consequently, the LFC controller alone attempts to restore the nominal frequency without assistance from the storage devices or intelligent demand-side management. The resulting frequency response, generated power, and power imbalance are recorded to establish the reference performance of the interconnected system.

The second simulation case employs the same interconnected renewable-based microgrid–multi-nanogrid configuration and identical initial operating conditions as those considered in Case 1. The same load disturbance is applied to ensure a fair comparison. In this case, the proposed coordinated DMS-UFLS strategy is activated together with the conventional LFC loop, while the RFB and STEP actively participate in system regulation by rapidly absorbing surplus renewable power or supplying the network during generation deficits. Immediately after the disturbance, the coordinated energy management strategy determines the optimal contribution of the available renewable sources and storage devices to minimize the generation–load mismatch and mitigate frequency deviations. If the available storage capacity becomes insufficient to maintain system stability, the optimized DMS-UFLS algorithm sequentially disconnects non-critical loads according to the optimal priority coefficients, beginning with external loads and, when necessary, extending to lower-priority loads within the EV charging, desalination, and STEP nanogrids. The

10.22060/EEJ.2026.26056.6045

coordinated operation of the PV arrays, wind turbines, CSP plant, RFB, and interconnected nanogrids is then assessed in terms of frequency regulation, power tracking capability, and reduction of the generation–load imbalance.

4.1 . Frequency Control in Interconnected Multi-Microgrid-Nanogrid

In this part, an optimal strategy for microgrid (MG) connected to several nanogrids (NG) was simulated. The aim was to test the optimal approach based on a bidirectional connection between a central microgrid and three independent nanogrids, in order to improve the robustness, stability and energy efficiency of the overall system. The microgrid was connected to three nanogrids, each having specific charge characteristics. This organization allows for greater flexibility in energy management and a rapid response to load fluctuations. The three nanogrids are defined as follows:

- 1st Nanogrid: *Electric vehicles.*

This nanogrid is mainly intended for charging EVs. Energy consumption was therefore highly variable and dependent on the recharging cycles, all electric motors of EVs are powered by variable frequency sinusoidal alternating current power electronics, adjustable to the network frequency at 50 Hz.

- 2nd Nanogrid: *Pumped Energy Transfer Station* .

This nanogrid was associated with a pumping system for hydraulic energy storage. It serves as a shock absorber to absorb surplus production, the transfer of energy by hydraulic pumping is the most mature technique of stationary storage. These installations contribute to maintaining the balance between generation and consumption on the electricity grid, while limiting production costs during peak consumption.

- 3rd Nanogrid: *Desalination Station*.

This nanogrid was intended to supply a seawater desalination station. This load is relatively constant but remains highly energy-consuming.

In this part, only the LFC loop is activated. The obtained results are presented in Fig.5 and Fig .6.

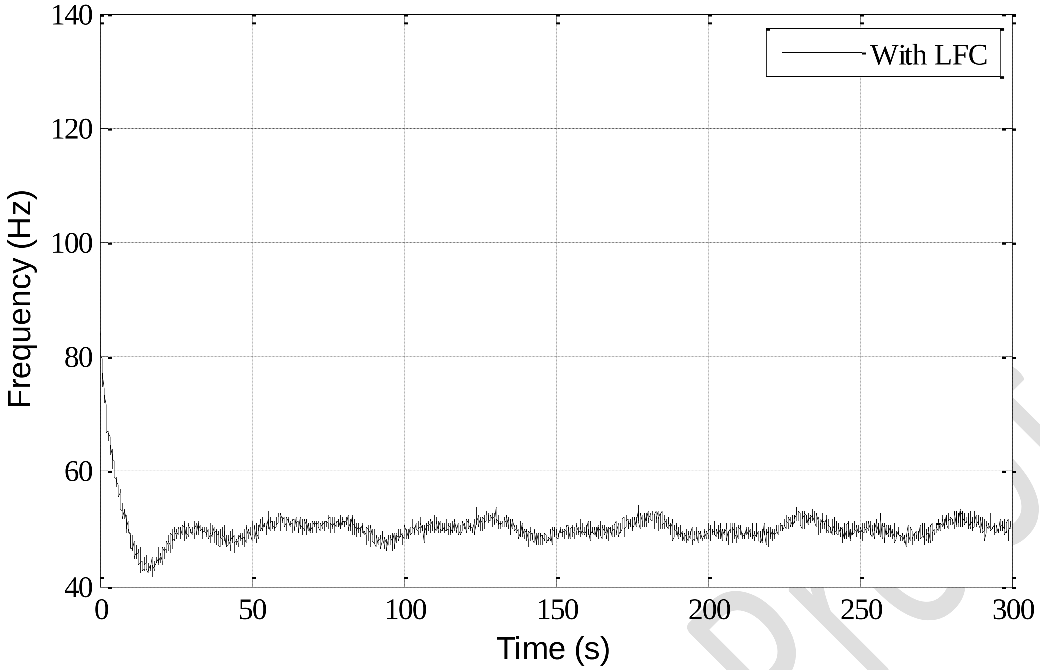

Fig 5. Microgrid Frequency.

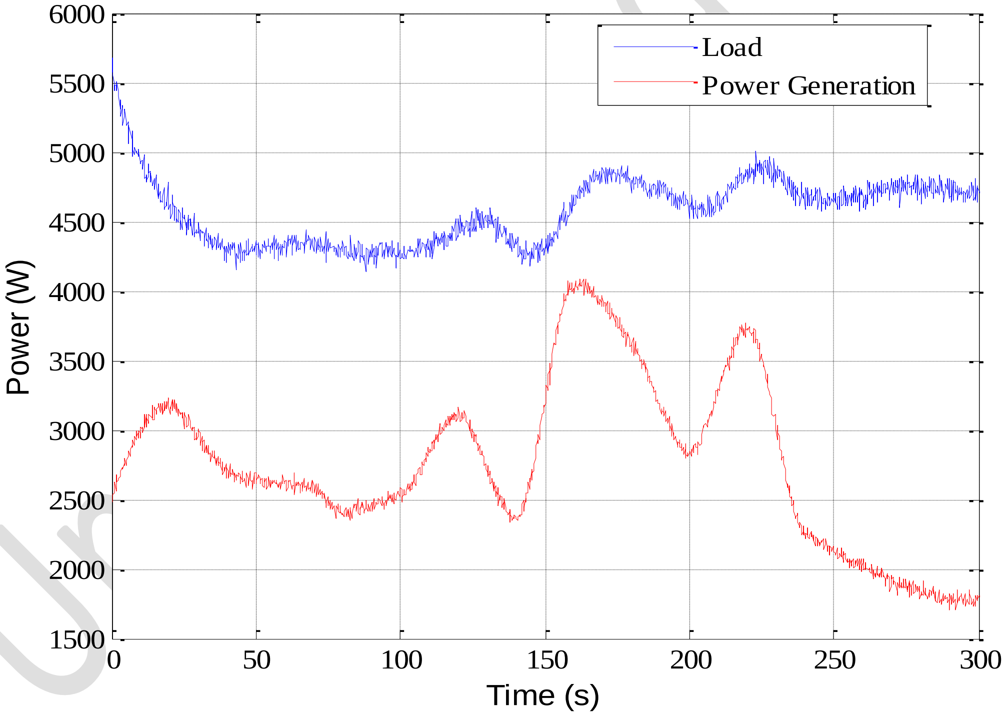

Fig 6. Microgrid Generated Power and Load Before UFLS.

In this simulation, it can be observed that the evolution of the frequency of the system presented in Fig.5, after the start of the microgrid. The objective was to check how the frequency stabilizes. The graph shows that at the very beginning, the frequency deviation was important, which is normal during the start-up phase because the system is not yet balanced. Very quickly, the frequency drops to stabilize around 50 Hz, which is the nominal value expected for correct operation of the electrical network. It can be seen that, despite

10.22060/EEJ.2026.26056.6045

some small oscillations around 50 Hz, the frequency remains globally stable throughout the simulation. These small variations are due to load changes. This result shows that the control strategy used makes it possible to efficiently return the frequency to its nominal value after the initial disturbances, thus ensuring stable and reliable operation of the microgrid. Further, it can be noticed the evolution of the frequency of the system without energy storage. The objective was to see how the microgrid reacts to load variations only with available renewable sources, without storage support. In Fig.6, the graph shows that the power generated P_g does not correctly follow the power consumed P_{load}. This shift results in a more pronounced instability of the frequency, because renewable energies, by their intermittency, cannot respond instantaneously to variations in load. Thus, the absence of storage directly impacts the stability of the network, and the system becomes less robust in the face of disturbances.

4.2 . Contribution of ESS to enhance Optimal DMS-UFLS Method

In this simulation, a load shedding strategy based on optimal coefficients called gains (denoted k1 to k6) was implemented. The idea is simple: in the event of a loss of production or a sharp increase in demand, it is necessary to know which loads to cut first to prevent the whole system from becoming unbalanced. In concrete terms, the charges have been divided into two main categories:

- External loads: These are loads connected directly to the main microgrid (e.g. non-essential buildings or secondary equipment).
- Inner loads: These are the loads that are inside the nanogrids (such as water pumping, electric vehicle charging or desalination).

The principle is that if ever there is a lack of power, the system will first shed the external loads (Switch OFF: k1, k2, k3). If this is not enough to restore balance, then some internal loads (Switch OFF: k4, k5, k6) will begin to be shedding, starting with those that are the least critical. The combined DMS-UFLS was named as EMS method during the simulation as presented in Figs 7, 8 and 9.

10.22060/EEJ.2026.26056.6045

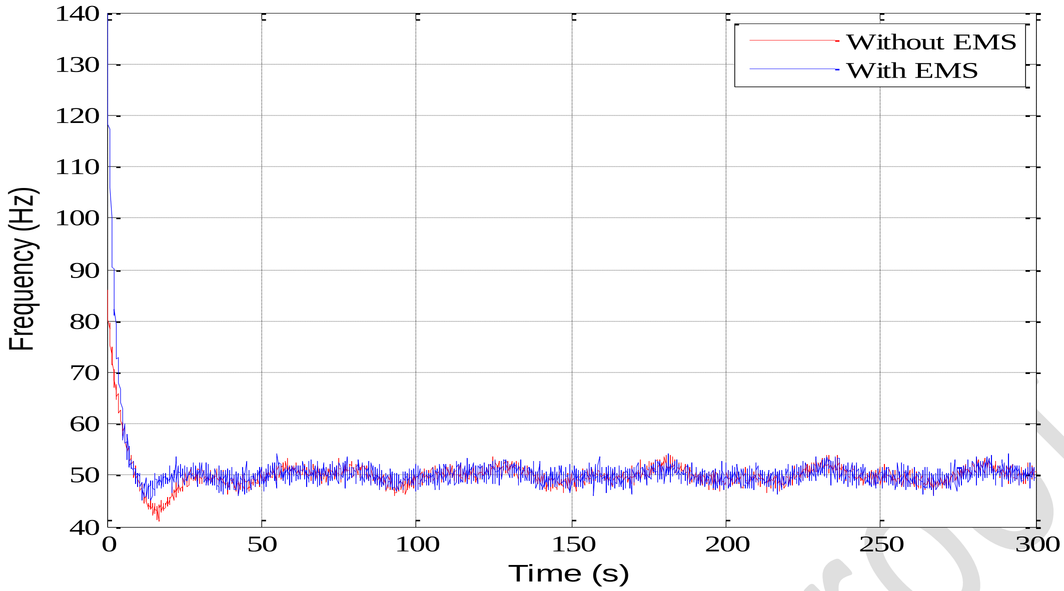

Fig 7. Microgrid Frequency.

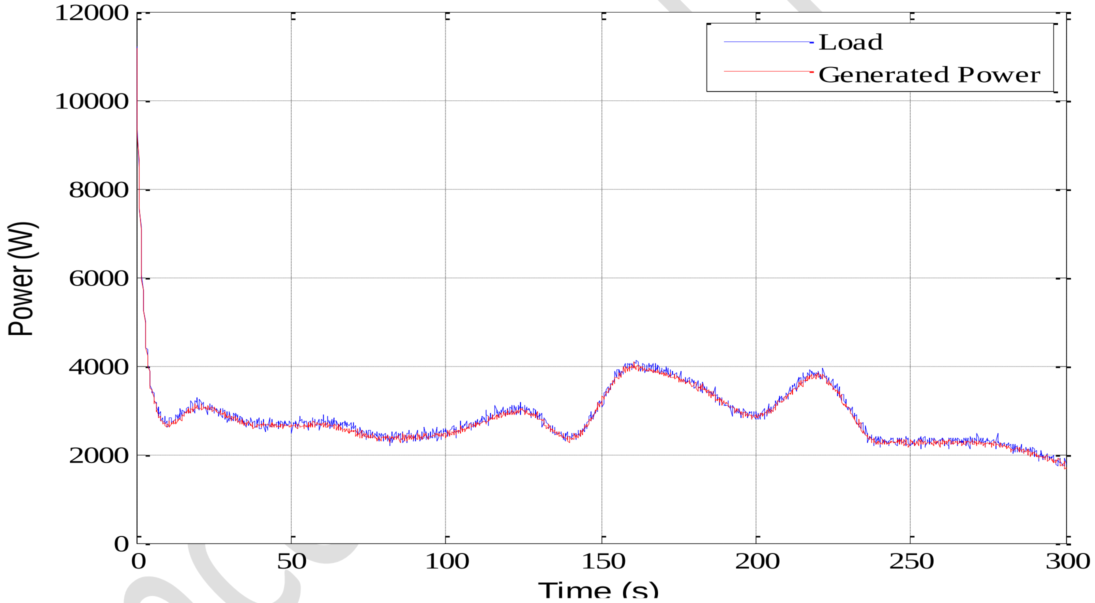

Fig 8. Microgrid Generated Power and Load Using Optimal DMS-UFLS.

10.22060/EEJ.2026.26056.6045

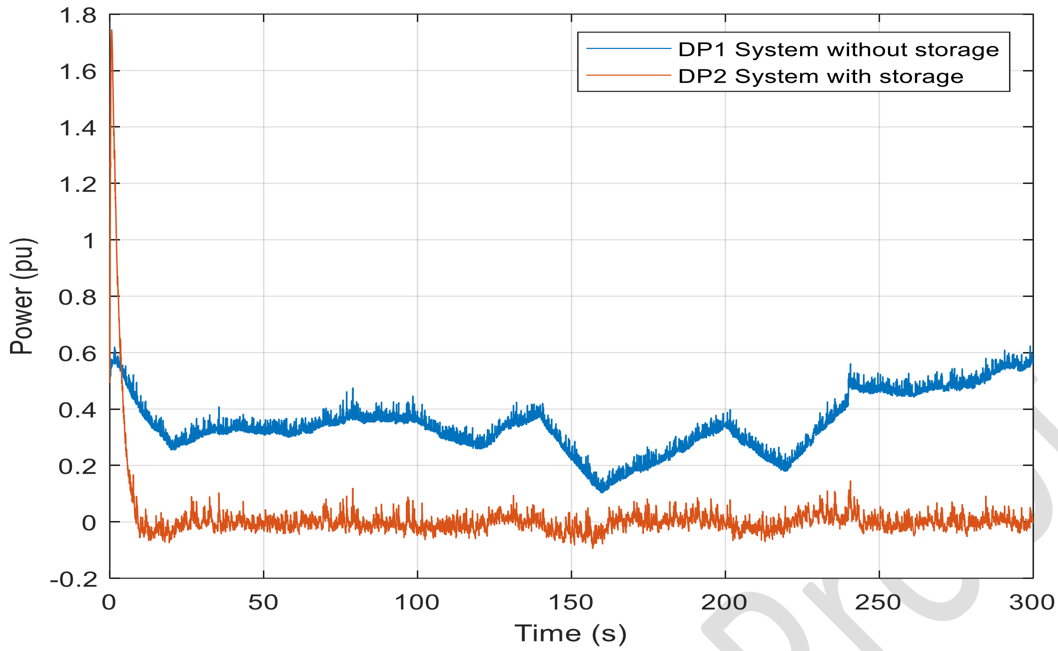

Fig 9. Microgrid Power Deviation.

In this second simulation, the proposed optimal DMS-UFLS involving LFC loop and ESS was presented. The aim was to compare the effect of storage on energy stability and microgrid dynamic response. The depicted graphs in Fig .7 clearly show that the power generated follows much better the power consumed compared to the previous case. Thanks to the energy storage system, the ESS is able to absorb surpluses or supply microgrid when it lacks renewable production. The frequency remains much more stable around 50 Hz, which proves that storage improves the network's ability to balance load and production. This confirms the importance of integrating storage into a highly renewable penetration microgrid.

In Fig .9, the graph shows that in the case without storage (blue curve), there are strong power oscillations, and P_g is not equal to P_{load} as presented in Fig .6. Management becomes more difficult, and the network is subject to risks of imbalance. On the other hand, in the case with storage (red curve), there is a better balance: the difference between production and consumption is almost zero as presented in Fig.8.This confirms that storage plays an essential role in maintaining stability and reducing discrepancies, allowing a smoother and continuous management of the load compared to production.

The results showed that without load shedding, the system can quickly be subjected to overloads, endangering the stability of the network. On the other hand, the introduction of a DMS with load shedding makes it possible to maintain the balance between load and production, to improve the stability of the frequency and to limit the disturbances. Thus, intelligent load shedding is an effective solution to guarantee the performance and reliability of multi-load nanogrids, by dynamically adapting to variations in consumption and production.

6. FUTURE WORK

Future work will focus on extending the proposed methodology toward multi-objective optimization considering economic and environmental criteria, integrating forecasting techniques based on artificial intelligence, and validating under real-time hardware-in-the-loop and cyber-physical system environments. In particular, In the near future this work will be extended to experimental validation of the proposed coordinated LFC–DMS/UFLS strategy, consideration of larger and more complex interconnected microgrids and nanogrids configurations, incorporation of additional uncertainties associated with renewable-energy generation and load demand. Furthermore, modern control and optimization algorithms, advanced energy-storage technologies, and peer-to-peer energy management will be investigated to further enhance the flexibility and resilience of the proposed framework.

7. CONCLUSION

This paper presented a novel bi-level optimization framework for distributed power management and intelligent load shedding in an islanded microgrid interconnected with multiple nanogrids under renewable energy variability. The proposed strategy combines an optimal Fuzzy-PID based LFC scheme tuned using the african vultures optimization algorithm with a coordinated DMS and intelligent UFLS mechanism. The developed architecture enables effective coordination between renewable generation units, energy storage systems, and multiple nanogrid loads. Simulation studies carried out under various operating conditions demonstrated the effectiveness of the proposed approach in maintaining the power balance and enhancing frequency stability despite the intermittent nature of renewable energy sources. The obtained results showed that the integration of ESS significantly reduces active power mismatches and mitigates frequency deviations, while the optimized Fuzzy-PID controller provides superior dynamic performance compared to conventional control schemes in terms of overshoot reduction and settling time.

Data availability: Data will be made available on request.

References

[1] SATTAR, Faisal, GHOSH, Sudipta, ISBEIH, Younes J., *et al.* A predictive tool for power system operators to ensure frequency stability for power grids with renewable energy integration. *Applied Energy*, 2024, vol. 353, p. 122226.

[2] HADAVI, Abolfazl, HAGH, Mehrdad Tarafdar, et ZADEH, Saeid Ghassem. Frequency Stability in Modern Power Systems with 100% Renewable Energy Penetration. *Results in Engineering*, 2025, p. 108168.

[3] UPADHAYA, Debodyuti, BISWAS, Soumen, DUTTA, Susanta, *et al.* Optimal power flow and grid frequency control of conventional and renewable energy source using evolutionary algorithm based FOPID controller. *Renewable Energy Focus*, 2025, vol. 53, p. 100676.
[4] ALAM, Md Shafiul, CHOWDHURY, Tanzi Ahmed, DHAR, Abhishak, *et al.* Solar and wind energy integrated system frequency control: A critical review on recent developments. *Energies*, 2023, vol. 16, no 2, p. 812.
[5] NJOKA, Godfrey Macharia, MOGAKA, Lucas, et WANGAI, Agnes. Impact of variable renewable energy sources on the power system frequency stability and system inertia. *Energy Reports*, 2024, vol. 12, p. 4983-4997.
[6] BINDU, Shilpa, SIGRIST, Lukas, et AVILA, Jose Pablo Chaves. Frequency stability services to compensate for low inertia in renewable-dominated power systems. *Utilities Policy*, 2025, vol. 95, p. 101938.
[7] HU, Jiefeng (ed.). *Community Energy and Microgrids: Control, Operation and Optimization*. Springer, 2024.
[8] LIAQAT, Nouman, CHIHAOUI, Naceur, NASIR, Muhammad, *et al.* Protection challenges and emerging solutions in renewable-integrated microgrids: a critical review. *Energy Informatics*, 2026, vol. 9, no 1, p. 24.
[9] RODRIGUEZ-GIL, Jhojan A., MOJICA-NAVA, Eduardo, VARGAS-MEDINA, Daniel, *et al.* Energy management system in networked microgrids: an overview: JA Rodriguez-Gil et al. *Energy Systems*, 2026, vol. 17, no 1, p. 315-346.
[10] NEDA, Omar Muhammed, ADABI, Jafar, MARZBAND, Mousa, *et al.* Hierarchical energy management system for coordinated operation of multiple grid-tied home microgrids. *Renewable Energy Focus*, 2025, p. 100766.
[11] BITAR, Maria, EL TAWIL, Tony, BENBOUZID, Mohamed, *et al.* On hybrid nanogrids energy management systems—an insight into embedded systems. *Applied Sciences*, 2024, vol. 14, no 4, p. 1563.
[12] DAHIRU, Ahmed Tijjani, DAUD, Dzurllkanian, TAN, Chee Wei, *et al.* A comprehensive review of demand side management in distributed grids based on real estate perspectives. *Environmental science and pollution research*, 2023, vol. 30, no 34, p. 81984-82013.
[13] YIM, Jaeyun, YOU, Sesun, BLAABJERG, Frede, *et al.* Energy management systems for forecasted demand error compensation using hybrid energy storage system in nanogrid. *Renewable Energy*, 2024, vol. 221, p. 119744.
[14] MAGDY, Gaber, BAKEER, Abualkasim, BAKEER, Mahmoud, *et al.* A new intelligent approach for frequency controller of autonomous hybrid power systems. *Neural Computing and Applications*, 2025, vol. 37, no 22, p. 17473-17492.
[15] WANG, Yang et XIONG, Guojiang. Metaheuristic optimization algorithms for multi-area economic dispatch of power systems: Part I—a comprehensive survey. *Artificial Intelligence Review*, 2025, vol. 58, no 4, p. 98.
[16] AHMAD, Ghali, SHAFIULLAH, Md, ZAERY, Mohamed, *et al.* Intelligent LFC for multi-microgrid system integrating ASIC and BESS. *Renewable Energy Focus*, 2026, p. 100817.
[17] LIU, Chenyuan, LI, Heng, LI, Kexin, *et al.* Deep learning for state of health estimation of lithium-ion batteries in electric vehicles: A systematic review. *Energies*, 2025, vol. 18, no 6, p. 1463.
[18] CHEMALI, Ephrem, KOLLMEYER, Phillip J., PREINDL, Matthias, *et al.* State-of-charge estimation of Li-ion batteries using deep neural networks: A machine learning approach. *Journal of power sources*, 2018, vol. 400, p. 242-255.
[19] WANG, Wenwen, WANG, Jun, TIAN, Jinpeng, *et al.* Application of digital twin in smart battery management systems. *Chinese Journal of Mechanical Engineering*, 2021, vol. 34, no 1, p. 57.
[20] ZHANG, Tai et STRBAC, Goran. Artificial intelligence applications for energy storage: A comprehensive review. *Energies*, 2025, vol. 18, no 17, p. 4718.
[21] JAMAL, Saif, PASUPULETI, Jagadeesh, RAHMAT, Nur Azzammudin, *et al.* Energy management system for grid-connected Nanogrid during COVID-19. *Energies*, 2022, vol. 15, no 20, p. 7689.
[22] EL ZERK, Abdallah, OUASSAID, Mohammed, et ZIDANI, Youssef. Multi-agent system for decentralized energy management approach in collaborative microgrids. In : *2020 IEEE 7th International Conference on Engineering Technologies and Applied Sciences (ICETAS)*. IEEE, 2020. p. 1-6.
[23] ALI, Asad, FAKHAR, Muhammad Salman, KASHIF, Syed Abdul Rahman, *et al.* Optimal scheduling of neural network-based estimated renewable energy nanogrid. *Energies*, 2022, vol. 15, no 23, p. 8933.
[24] MOGA, Olimpiu Nicolae, FLOREA, Adrian, SOLEA, Claudiu, *et al.* Reinforcement Learning-Based Energy Management in Community Microgrids: A Comparative Study. *Sustainability*, 2025, vol. 17, no 23, p. 10696.
[25] KIASARI, Mahmoud et ALY, Hamed. AI-Driven Control Strategies for FACTS Devices in Power Quality Management: A Comprehensive Review. *Applied Sciences (2076-3417)*, 2025, vol. 15, no 22.
[26] NGEI, Urbanus Mwanzia, NYETE, Abraham Mutunga, MOSES, Peter Musau, *et al.* Optimal sizing and placement of STATCOM, TCSC and UPFC using a novel hybrid genetic algorithm-improved particle swarm optimization. *Heliyon*, 2024, vol. 10, no 23.

[27] A. S. Kannan, “Hybrid AI-Optimized FACTS Controllers for Enhancing Small-Signal and Transient Stability in Multi-Machine Power Systems,” *J. Electr. Syst.*, vol. 21, no. 01, pp. 1203–1235, Feb. 2025.

[28] MAROUANI, Ismail, GUESMI, Tawfik, ALSHAMMARI, Badr M., *et al.* Optimized FACTS devices for power system enhancement: applications and solving methods. *Sustainability*, 2023, vol. 15, no 12, p. 9348.

[29] ÖZKAYA, Burçin. Optimization of optimal power flow considering location of facts devices using partial reinforcement optimizer. *European Journal of Technique (EJT)*, 2024, vol. 14, no 1, p. 51-61.

[30] HARRISON, Ambe, FENDZI MBASSO, Wulfran, KUMAR, Raman, *et al.* Probabilistic deep learning control of hybrid FACTS for real-time voltage stability in renewable-rich power grids. *International Journal of Dynamics and Control*, 2026, vol. 14, no 2, p. 59.

[31] ALJAIDI, Mohammad, JANGIR, Pradeep, AGRAWAL, Sunilkumar P., *et al.* Optimizing FACTS device placement using the Fata Morgana algorithm: A cost and power loss minimization approach in uncertain load Scenario-Based systems. *International Journal of Computational Intelligence Systems*, 2025, vol. 18, no 1, p. 12.

[32] VILLALVA, Marcelo Gradella, GAZOLI, Jonas Rafael, et RUPPERT FILHO, Ernesto. Comprehensive approach to modeling and simulation of photovoltaic arrays. *IEEE Transactions on power electronics*, 2009, vol. 24, no 5, p. 1198-1208.

[33]J. S. Ali, Y. Qiblawey, A. Alassi, A. M. Massoud, S. M. Muyeen and H. Abu-Rub, "Power System Stability With High Penetration of Renewable Energy Sources: Challenges, Assessment, and Mitigation Strategies," in *IEEE Access*, vol. 13, pp. 39912-39934, 2025, doi: 10.1109/ACCESS.2025.3546491.

[34] DE SOTO, Widalys, KLEIN, Sanford A., et BECKMAN, William A. Improvement and validation of a model for photovoltaic array performance. *Solar energy*, 2006, vol. 80, no 1, p. 78-88.

[35] ISHAQUE, Kashif, SALAM, Zainal, MEKHILEF, Saad, *et al.* Parameter extraction of solar photovoltaic modules using penalty-based differential evolution. *Applied Energy*, 2012, vol. 99, p. 297-308.

[36] MÜLLER, Set, DEICKE, M., et DE DONCKER, Rik W. Doubly fed induction generator systems for wind turbines: A viable alternative to adjust speed over a wide range at minimal cost. *IEEE Industry applications magazine*, 2002, vol. 8, no 3, p. 26-33.

[37] PENA, R., CLARE, J. C., et ASHER, G. M. A doubly fed induction generator using back-to-back PWM converters supplying an isolated load from a variable speed wind turbine. *IEE Proceedings-Electric Power Applications*, 1996, vol. 143, no 5, p. 380-387.

[38] ABAD, Gonzalo, LOPEZ, Jesus, RODRIGUEZ, Miguel, *et al. Doubly fed induction machine: modeling and control for wind energy generation*. John Wiley & Sons, 2011.

[39] WEBER, Adam Z., MENCH, Matthew M., MEYERS, Jeremy P., *et al.* Redox flow batteries: a review. *Journal of applied electrochemistry*, 2011, vol. 41, no 10, p. 1137-1164.

[40] SKYLLAS-KAZACOS, Maria, CHAKRABARTI, M. H., HAJIMOLANA, S. A., *et al.* Progress in flow battery research and development. *Journal of the electrochemical society*, 2011, vol. 158, no 8, p. R55-R79.

[41] ALOTTO, Piergiorgio, GUARNIERI, Massimo, et MORO, Federico. Redox flow batteries for the storage of renewable energy: A review. *Renewable and sustainable energy reviews*, 2014, vol. 29, p. 325-335.

[42] KEMPTON, Willett et TOMIĆ, Jasna. Vehicle-to-grid power fundamentals: Calculating capacity and net revenue. *Journal of power sources*, 2005, vol. 144, no 1, p. 268-279.

[43] GUILLE, Christophe et GROSS, George. A conceptual framework for the vehicle-to-grid (V2G) implementation. *Energy policy*, 2009, vol. 37, no 11, p. 4379-4390.

[44] DAI, Jianzhuo, DONG, Ming, YE, Rixin, *et al.* A review on electric vehicles and renewable energy synergies in smart grid. In : *2016 China International Conference on Electricity Distribution (CICED)*. IEEE, 2016. p. 1-4.

[45] GHAFFOUR, Noreddine, MISSIMER, Thomas M., et AMY, Gary L. Technical review and evaluation of the economics of water desalination: Current and future challenges for better water supply sustainability. *Desalination*, 2013, vol. 309, p. 197-207.

[46] CALDERA, Upeksha, BOGDANOV, Dmitrii, AFANASYEVA, Svetlana, *et al.* Role of seawater desalination in the management of an integrated water and 100% renewable energy based power sector in Saudi Arabia. *Water*, 2017, vol. 10, no 1, p. 3.

[47] SHAHZAD, Muhammad Wakil, BURHAN, Muhammad, YBYRAIYMKUL, Doskhan, *et al.* Desalination with renewable energy: A 24 hours operation solution. In : *Water and wastewater treatment*. IntechOpen, 2019.

[48] K. Nour El Yakine, A. Boudoucha, and A. Brik, “Optimal sustainable marine microgrid control using seawater desalination station and pumped storage system for smoothing offshore power fluctuation,” presented at the Conference: International Conference on Engineering Sciences, Sfax, Tunisia, Jun. 2025.

[49] Nour El Yakine, Kouba, Bouziane, Boussahoua, Toufik, Tarif, Djamel, Selkim, and Radia, Matki, “Smart Monitoring of Marine Microgrid Connected Seawater Desalination Station to Supply Shipboard and Airport,”

10.22060/EEJ.2026.26056.6045

presented at the 9th International Conference on Artificial Intelligence in Renewable Energetic Systems, IC-AIRES2025, Mostaganem, Algeria, Oct. 2025.
[50] YANG, Chi-Jen. Pumped hydroelectric storage. In : *Storing energy*. Elsevier, 2016. p. 25-38.
[51] REHMAN, Shafiqur, AL-HADHRAMI, Luai M., et ALAM, Md Mahbub. Pumped hydro energy storage system: A technological review. *Renewable and Sustainable Energy Reviews*, 2015, vol. 44, p. 586-598.
[52] KOUGIAS, Ioannis et SZABÓ, Sándor. Pumped hydroelectric storage utilization assessment: Forerunner of renewable energy integration or Trojan horse?. *Energy*, 2017, vol. 140, p. 318-329.
[53] CHETHAN, Muddu et KUPPAN, Ravi. A review of FACTS device implementation in power systems using optimization techniques. *Journal of Engineering and Applied Science*, 2024, vol. 71, no 1, p. 18.

Appendix

Table A.1. Simulation parameters.

Component	Parameters
PV array	$K_{PV1} = 1$, $T_{PV1} = 1.8$
STEP	$K_{STEP} = 5$, $T_{STEP} = 2.3$
EVs	$K_{EVs} = 0.01$, $T_{EVs} = 0.5$
CSP	$K_{CSP} = 1$, $T_{CSP} = 1.8$
Wind farm	$K_{WT,off2} = 0.8$, $T_{WT,off2} = 10$
RFB	$K_{RFB4} = 1$, $T_{RFB4} = 1.8$

10.22060/EEJ.2026.26056.6045

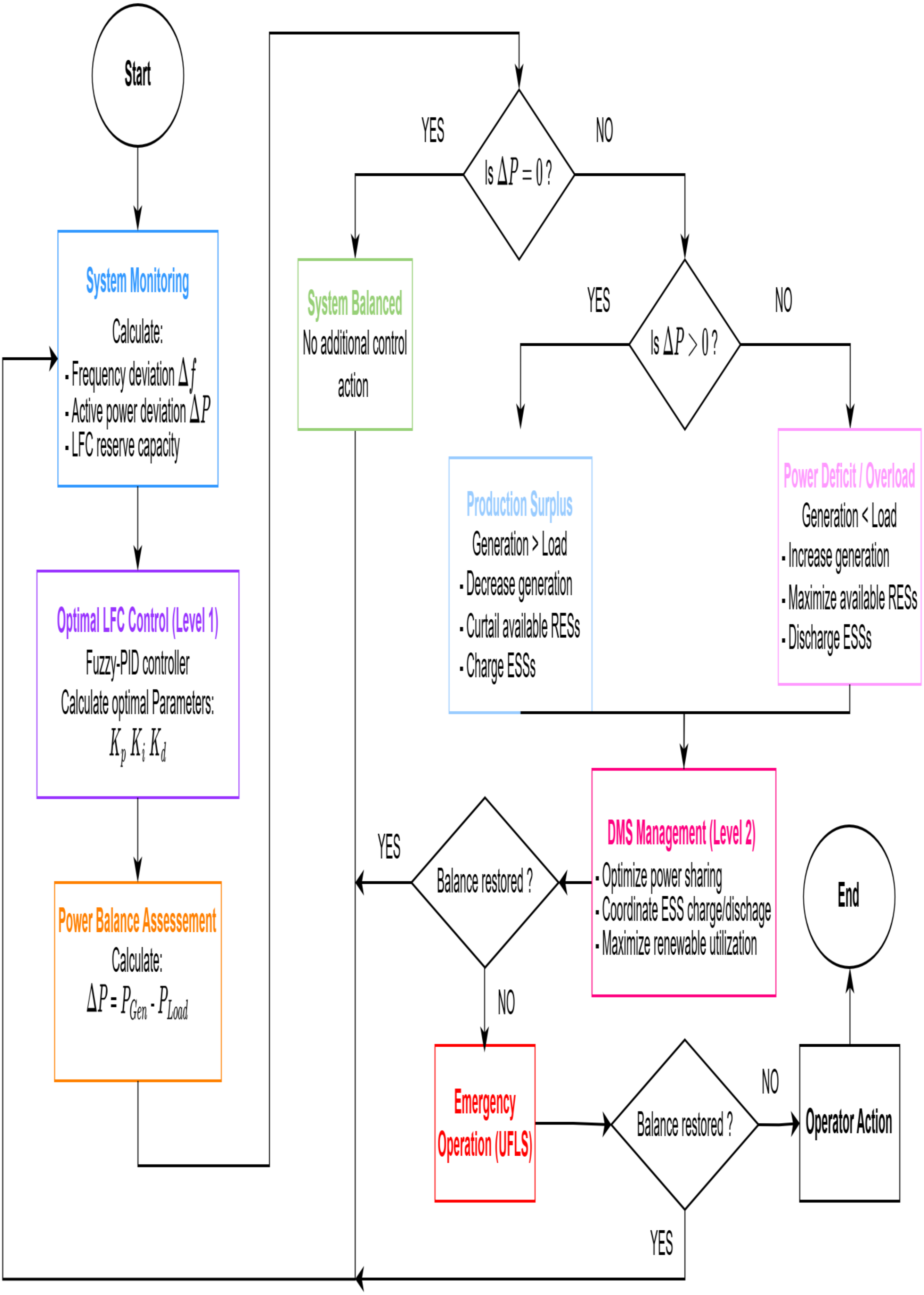

AUT Journal of Electrical Engineering
10.22060/EEJ.2026.26056.6045

Fig. A.1. Flowchart of the Proposed Optimal DMS-UFLS.